

## Supplementary Information

### Mutation-specific dual potentiators maximize rescue of CFTR gating mutants

Guido Veit<sup>1</sup>, Dillon F. Da Fonte<sup>1</sup>, Radu G. Avramescu<sup>1</sup>, Aiswarya Premchandar<sup>1</sup>, Miklos Bagdany<sup>1</sup>, Haijin Xu<sup>1</sup>, Dennis Bensinger<sup>2</sup>, Daniel Stubba<sup>2</sup>, Boris Schmidt<sup>2</sup>, Elias Matouk<sup>3</sup> and Gergely L. Lukacs<sup>1,4</sup>

#### Correspondence:

Guido Veit  
Dept. of Physiology  
McGill University  
3655 Promenade Sir-William-Osler  
Montreal, QC, H3G 1Y6  
Canada  
Email: [guido.veit@mcgill.ca](mailto:guido.veit@mcgill.ca)

Gergely L. Lukacs  
Dept. of Physiology and Dept. of Biochemistry  
McGill University  
3655 Promenade Sir-William-Osler  
Montreal, QC, H3G 1Y6  
Canada  
Email: [gergely.lukacs@mcgill.ca](mailto:gergely.lukacs@mcgill.ca)

#### This file contains:

Supplementary Methods

Supplementary Fig. 1-7

Supplementary Tables 1-3

## Supplementary Methods

### Antibodies and reagents

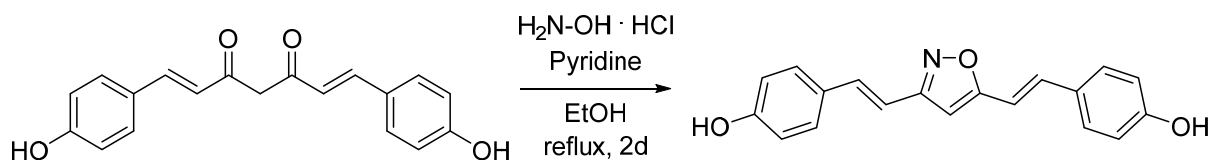
The following antibodies were used: Mouse monoclonal anti-hemagglutinin (HA) antibody (Biolegend, clone 16B12, 1:2000), mouse anti-acetylated tubulin (1:200, Sigma T7451), rabbit anti-zonula occludens-1 (1:100, Invitrogen 402200), mouse anti-mucin5AC (1:200, Thermo Scientific MA1-38223) and mouse anti-Na<sup>+</sup>/K<sup>+</sup>-ATPase (Santa Cruz Biotechnology, sc-48345, 1:5000). VX-770, VX-809 and ABBV-974 were purchased from Selleckchem. Bisdemethoxycurcumin and apigenin were from Sigma. The CFTR potentiators P1 to P10 were made available by R. J. Bridges (Rosalind Franklin University of Medicine and Science) and CFFT. A15 [1] was a kind gift of A.S. Verkman (University of California–San Francisco). Potentiators P12, C-01, D-01, E-01, F-01, H-01 and A-04 have been published previously [2].

### Curcumin analog synthesis

**General remarks.** All reactions requiring anhydrous conditions were performed in dried glassware under argon atmosphere. All reagents and solvents were obtained from commercial suppliers without further purification. NMR spectra were recorded with a Bruker DRX 500 (500 MHz <sup>1</sup>H, 126 MHz <sup>13</sup>C). Deuterated solvents were used as internal standard. The  $\delta$  values are reported in parts per million (ppm) downfield from TMS and were referenced to the residual solvent signal (DMSO-*d*<sub>6</sub>). Coupling constants *J* are given in Hertz (Hz). The spectra were analyzed using MestReNova 11 (Mestrelab Research). HPLC was performed using an Agilent 1100 system with a Phenomenex synergi polar reversed phase column (4  $\mu$ m particle size, 150 x 3.0 mm, pore size 80Å) connected to a variable wavelength detector. The mobile phase consists of water/acetonitrile + 0.1% trifluoro acetic acid forming a linear gradient starting with 30%

water (held for 1 min) increased to 90% acetonitrile within 10 min and held for 1 min with a constant flow of 1 mL/min. Flash chromatography was performed using a Teledyne ISCO Combiflash Rf 4x system with pre-packed silica columns obtained from Telos. The column was conditioned with solvent to the starting concentration of the gradient. Peaks were detected at 254/280 nm (normal phase chromatography). Thin-layer chromatography was carried out on 0.2 mm silica gel 60 plates (F-254 Merck). They were detected by UV light (254 and 365 nm). All compounds used in biochemical assays have a purity of more than 95% as determined by HPLC and are reported at the corresponding experiment. Bisdemethoxycurcumin was synthesized as described by Cao *et al.* [3].

#### **Synthesis of 4,4'-((1E,1'E)-isoxazole-3,5-diylbis(ethene-2,1-diyl))diphenol (C111)**



The title compound was prepared according to a modified procedure of Narlawar *et al.* [4]. To a stirred solution of bisdemethoxycurcumin (200 mg, 0.730 mmol, 1.0 eq.) in 5 mL of EtOH was added hydroxylamine hydrochloride (200 mg, 2.88 mmol, 3.9 eq.) and pyridine (220  $\mu$ L, 216 mg, 2.73 mmol, 3.7 eq.) and the reaction mixture was heated to reflux for 48 h. After completion of the reaction, the solvent was removed under reduced pressure and the crude product was purified by automated flash column chromatography (CH<sub>2</sub>Cl<sub>2</sub>/MeOH = 0 to 10%) to afford the title compound as a white solid (31 mg, 0.102 mmol, 14%)

**HPLC** (254 nm, VWD):  $t_R$  = 6.10 min (96.10%).

**<sup>1</sup>H-NMR** (500 MHz, DMSO-*d*<sub>6</sub>):  $\delta$  = 9.58 (s, 1H), 9.51 (s, 1H), 7.41 – 7.35 (m, 4H), 7.21 (d, *J* = 16.4 Hz, 1H), 7.15 (d, *J* = 16.4 Hz, 1H), 6.87 (d, *J* = 11.1 Hz, 1H), 6.83 (d, *J* = 11.1 Hz, 1H), 6.77 (dd, *J* = 8.6, 2.5 Hz, 4H), 6.63 (s, 1H).

**<sup>13</sup>C-NMR** (126 MHz, DMSO-*d*<sub>6</sub>):  $\delta$  = 168.0, 161.8, 158.5, 158.2, 135.6, 134.1, 128.4, 128.1, 126.5, 126.2, 115.6, 115.5, 112.1, 109.7, 97.4.

### **Cell lines**

The generation of CFBE41o- (CFBE) cell lines expressing inducible CFTR variants has been described previously [5]. CFBE cells were maintained in MEM medium (Invitrogen) supplemented with 10% fetal bovine serum, 2 mM L-glutamine and 10 mM 4-(2-hydroxyethyl)-1-piperazineethanesulfonic acid (HEPES) on human fibronectin-coated plastic dishes. For experiments CFBE were seeded at a density of  $2 \times 10^4$  cells/ well into 96 well plates or  $1 \times 10^5$  cell/filter on 1.12 cm<sup>2</sup> Snapwell filter supports (Corning) and the expression of CFTR variants was induced for  $\geq 3$  days with 50-500 ng/ml doxycycline.

### **Human bronchial and nasal epithelia**

HNE from two CF patients (genotypes G551D/F508del and S549R/F508del) and five non-diseased WT donors were isolated following the protocol and consent form approved by the McGill MUHC Research Ethics Board (MP-37-2018-4227). HNE from one CF patient (genotype G551D/Y1092X) and human bronchial epithelia (HBE) isolated from the bronchi following lung transplantation of homozygous F508del CF individuals (CFBE 13-35) were a gift from W. Finkbeiner (University of California-San Francisco). Other HNE (genotype G551D/G551D) or HBE (BCF130409, BCF121209 and BCF060314, genotype F508del/F508del) were purchased

from the Cystic Fibrosis Canada-Sick Kids Program in Individual CF Therapy and the Cystic Fibrosis Translational Research center (CFTRc) at McGill University, respectively.

HNE were isolated from scrape biopsies of the upper nasal turbinates following an established protocol [6]. Cells were expanded using the conditional reprogramming technique [7] by co-culturing with irradiated 3T3-J2 fibroblasts in presence of ROCK inhibitor (10  $\mu$ M Y-27632). For functional measurements, cells were seeded at a density of  $5 \times 10^5$  cell/filter on 1.12  $\text{cm}^2$  Snapwell filter supports (Corning) and differentiated under air-liquid interface by culturing in Ultrosor G (Pall Corporation) containing medium for  $\geq$  four weeks for HBE [8] or by culturing in PneumaCult-ALI medium (Stemcell Technologies) for  $\geq$  three weeks for HNE. Interestingly, differentiation in PneumaCult-ALI medium supported a forskolin-stimulated WT-CFTR current in HNE of  $44 \pm 3 \mu\text{A}/\text{cm}^2$  compared to the previously reported  $16 \pm 3 \mu\text{A}/\text{cm}^2 I_{\text{sc}}$  of WT-CFTR in HNE differentiated in Ultrosor G containing medium [9].

### **PM density measurement**

The PM density of 3HA-tagged CFTR variants was determined by cell surface enzyme-linked immunosorbent assay (ELISA) [10]. PM density measurements were normalized with alamarBlue cell viability assay (Invitrogen).

### **Short-circuit current measurement**

Short-circuit current measurement of polarized CFBE [5] and HBE [11] has been described previously. The Snapwell filter grown cells were mounted in Ussing chambers (Physiologic Instruments) in Krebs-bicarbonate Ringer (KBR) buffer (140 mM  $\text{Na}^+$ , 120 mM  $\text{Cl}^-$ , 5.2 mM  $\text{K}^+$ , 25 mM  $\text{HCO}_3^-$ , 2.4 mM  $\text{HPO}_4$ , 0.4 mM  $\text{H}_2\text{PO}_4$ , 1.2 mM  $\text{Ca}^{2+}$ , 1.2 mM  $\text{Mg}^{2+}$ , 5 mM glucose, pH

7.4), which was mixed by bubbling with carbogen (95% O<sub>2</sub> and 5% CO<sub>2</sub>). CFBE and HNE were measured in presence of basolateral-to-apical chloride gradient, generated by replacing NaCl with Na<sup>+</sup> gluconate in the apical buffer. For CFBE epithelia the basolateral membrane was permeabilized with 100 μM amphotericin B (Sigma-Aldrich). After compensating for voltage offsets, the transepithelial voltage was clamped at 0 mV and measurements were recorded at 37°C in the presence of 100 μM amiloride with the Acquire and Analyze package (Physiologic Instruments).

### **Halide-sensitive YFP quenching assay**

CFTR function measurement by halide-sensitive YFP quenching assay was performed as described previously [5]. Briefly, CFBE cells harbouring the inducible expression of CFTR variants were generated to co-express the halide sensor YFP-F46L/H148Q/I152L [12] by lentiviral transduction. During the assay, YFP-expressing CFBE cells were incubated at 32°C in 50 μl per well phosphate-buffered saline (PBS)-chloride (140 mM NaCl, 2.7 mM KCl, 8.1 mM Na<sub>2</sub>HPO<sub>4</sub>, 1.5 mM KH<sub>2</sub>PO<sub>4</sub>, 1.1 mM MgCl<sub>2</sub>, 0.7 mM CaCl<sub>2</sub>, and 5 mM glucose, pH 7.4) containing potentiator compounds. Well-by-well measurements were performed. CFTR was activated by 50 μl injection of activator solution [20 μM forskolin, 0.5 mM 3-isobutyl-1-methyl-xanthine (IBMX), 0.5 mM 8-(4-chlorophenylthio)-adenosine-3',5'-cyclic monophosphate (cpt-cAMP)] in PBS-chloride at 0 seconds. By injecting 100 μl of PBS-iodide, in which NaCl was replaced with NaI, the quenching reaction was started at 60 seconds. With a 5-Hz data acquisition rate the YFP-fluorescence (485-nm excitation and 520-nm emission) was recorded between 57 and 93 seconds in a POLARstar OPTIMA (BMG Labtech) fluorescence plate reader. After background values were subtracted, the YFP signal was normalized to the fluorescence

before NaI injection. To exclude the instantaneous quenching artifact upon NaI injection during the first second, the influx rates were calculated by linear fitting to the initial slope starting from 61 seconds

### **Reconstitution CFTR channel activity in lack lipid membrane (BLM)**

Microsomes containing WT- or G551D-CFTR were isolated from stably transfected BHK-21 cell and reconstituted in BLM as described [13]. The planar lipid bilayer was painted at a 2:1 ratio of 1-palmitoyl-2-oleoyl-sn-glycero-3-phosphoethanolamine (POPE) and 1-palmitoyl-2-oleoyl-sn-glycero-3-phospho-L-serine (POPS) (Avanti Lipids) at 25 mg/ml final lipid concentration dissolved in n-decane. Cis and trans cups contained 0.8-1 ml symmetrical buffer solutions (300 mM Tris-HCl, 10 mM HEPES (pH 7.2), 5 mM MgCl<sub>2</sub>, and 1 mM EGTA) with or without potentiators. In addition, the cis-side cup contained 2 mM ATP and 100 U/ml PKA catalytic subunit (Promega). The activity of the phosphorylated G551D-CFTR was confirmed by recording the I/V relationship in presence of VX-770.

To determine the effect of dual potentiator treatment, CFTR currents were measured by at -60 mV holding potential and a temperature of 28-30°C. Signals were low pass filtered at 200 Hz by an 8-pole Bessel filter, and digitized at 10 kHz by Digidata 1320 (Axon Instruments). The open probability ( $P_o$ ) of the channels was determined after digitally filtering at 50 Hz by analysis of records with the Clampfit 10.3 software.

### **Affinity purification of HBH-tagged CFTR variants**

The HBH-CFTR-3HA variants were expressed and affinity-purified as described previously [14]. Briefly, CFBE monolayers expressing HBH-S549N-CFTR-3HA and HBH-G551D-CFTR-3HA

were grown on fibronectin-coated 6-cm dishes and induced with doxycycline (250 ng/ml) for four days post-confluency. After treatments (20 $\mu$ M forskolin, 5 min; 3 $\mu$ M VX-770, 5 min; 50  $\mu$ M genistein, 5 min in KRB at 37°C), cells were washed and lysed with lysis buffer (0.4% Triton X-100, 300 mM NaCl; 20 mM Tris pH 8.0, 1 mM DTT) supplemented with protease inhibitors, kinase inhibitors, and phosphatase inhibitors. The lysate supernatant was bound to Dynabeads® MyOne™ Streptavidin C1 (Thermo Fischer Scientific), followed by a series of extensive washes. The bead-bound protein samples were kept in 50 mM ammonium bicarbonate supplemented with 0.01% DMNG (Anatrace) until digestion.

### **Tryptic digestion and tandem mass spectrometry**

The on-bead tryptic digestion of the proteins was done as described previously [14], and the parameters of the LC-MS/MS setup was modified as described below. Peptides were eluted with a two-slope gradient at a flow rate of 250 nL/min. Solvent B first increased from 1 to 36% in 66 min and then from 36 to 90% B in 14 min. Nanospray and S-lens voltages were set to 1.3-1.8 kV and 50 V, respectively. The capillary temperature was set to 225°C. Full scan MS survey spectra (m/z 360-1560) in profile mode were acquired in the Orbitrap Fusion with a resolution of 120,000 and a target value at 1e6. The most intense peptide ions were fragmented by both HCD and EThcD and analyzed in the linear ion trap with a target value at 2e4, and normalized collision energy at 28 V. Whenever a neutral loss of phosphoric acid (48.99, 32.66 or 24.5 Th) was detected in the HCD MS2 scans, an MS3 scanning was performed. The duty cycle was set to 3 s, and target ions selected for fragmentation were dynamically excluded for 30 s after 3 MS/MS events.



### **Peptide identification and quantification of phospho-occupancy**

The peak list was generated with Proteome Discoverer (version 2.1) using the following parameters: mass range: 500 Da - 6000 Da, no MS/MS spectral grouping, precursor charge: auto, and the minimum number of fragment ions: 5. The data were searched against the UniProt human and user-defined CFTR mutant database using Mascot 2.6 (Matrix Science), with the mass tolerances for precursor and fragment ions set at 10 ppm and 0.6 Da, respectively. Other filters included one missed tryptic cleavage, fixed modifications of cysteine carbamidomethylation, and variable modification of methionine oxidation. Manual validation of phospho-peptides was performed using Scaffold (version 4.8). Phosphorylated and non-phosphorylated CFTR peptides were quantified using Pinnacle software (Optys Technologies). The file areas of each peptide were normalized between treatments to the total CFTR reads within each treatment group. The phospho-occupancy was calculated as a ratio of all phosphorylated and unphosphorylated peptides that contained a given phosphosite, i.e. % phosphorylation of site A = [area of peptides phosphorylated at site A / sum of areas of all peptides carrying site A]

### **qPCR**

QPCR to determine the expression level of CFTR in different cell lines and patient-derived cells was performed as described previously [5].

### **Immunostaining**

Filter-grown HNE were washed twice for 2 min at 37°C with PBS to remove excess mucins. Cells were fixed (4% PFA, 10 min), permeabilized (0.2% Triton X-100, 5 min) and blocked (0.5% BSA in PBS + 0.1 mM Ca<sup>2+</sup> + 1mM Mg<sup>2+</sup>, 1 h), followed by primary antibody incubation

overnight at 4°C. Cells were subsequently incubated with the following secondary antibodies at room temperature: mouse-A488 (1:1000, 1 h); rabbit-A555 (1:1000, 1 h). Nuclei were stained with DAPI (100 ng/ml, 10min). After washing (4 times, 5 min with PBS), the filter inserts were mounted between a glass slide and a coverslip and images were acquired with a Zeiss LSM 700 confocal microscope equipped with a Plan-Apochromat 63x/1.40 oil differential interference contrast objective.

### **Statistical analysis**

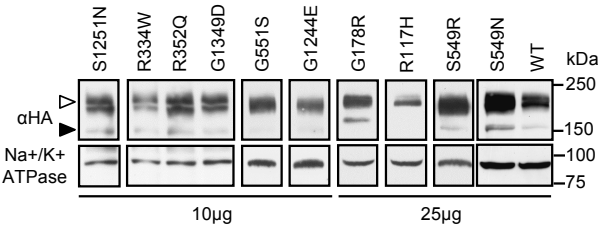
Unless otherwise specified, statistical analysis was performed by two-tailed Student's t-test with the means of at least three independent experiments and the 95% confidence level was considered significant. Dose-response plots were fitted with a pharmacological dose-response or bi-dose-response equation using OriginPro 8 or GraphPad Prism. Clustering was performed with the Heatmapper software (<http://www2.heatmapper.ca/>), using the average linkage method and distance calculation by Spearman's rank correlation.

### **References**

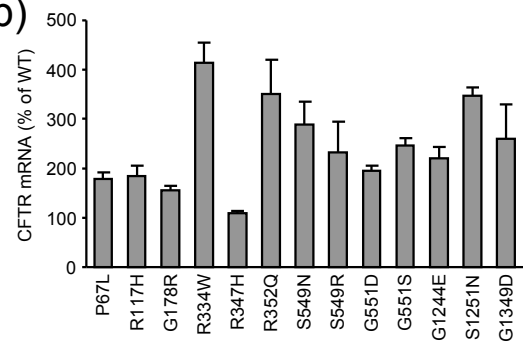
- [1] Haggie PM, Phuan PW, Tan JA, Xu H, Avramescu RG, Perdomo D, et al. Correctors and Potentiators Rescue Function of the Truncated W1282X-Cystic Fibrosis Transmembrane Regulator (CFTR) Translation Product. *J Biol Chem.* 2017;292:771-85.
- [2] Phuan PW, Veit G, Tan JA, Finkbeiner WE, Lukacs GL, Verkman AS. Potentiators of Defective DeltaF508-CFTR Gating that Do Not Interfere with Corrector Action. *Mol Pharmacol.* 2015;88:791-9.
- [3] Cao Y-K, Li H-J, Song Z-F, Li Y, Huai Q-Y. Synthesis and Biological Evaluation of Novel Curcuminoid Derivatives. *Molecules.* 2014;19:16349-72.
- [4] Narlawar R, Pickhardt M, Leuchtenberger S, Baumann K, Krause S, Dyrks T, et al. Curcumin-Derived Pyrazoles and Isoxazoles: Swiss Army Knives or Blunt Tools for Alzheimer's Disease? *ChemMedChem.* 2008;3:165-72.
- [5] Veit G, Bossard F, Goepf J, Verkman AS, Galiotta LJ, Hanrahan JW, et al. Proinflammatory cytokine secretion is suppressed by TMEM16A or CFTR channel activity in human cystic fibrosis bronchial epithelia. *Mol Biol Cell.* 2012;23:4188-202.

- [6] Muller L, Brighton LE, Carson JL, Fischer WA, 2nd, Jaspers I. Culturing of human nasal epithelial cells at the air liquid interface. *J Vis Exp*. 2013:e50646.
- [7] Liu X, Ory V, Chapman S, Yuan H, Albanese C, Kallakury B, et al. ROCK inhibitor and feeder cells induce the conditional reprogramming of epithelial cells. *Am J Pathol*. 2012;180:599-607.
- [8] Neuberger T, Burton B, Clark H, Van Goor F. Use of primary cultures of human bronchial epithelial cells isolated from cystic fibrosis patients for the pre-clinical testing of CFTR modulators. *Methods Mol Biol*. 2011;741:39-54.
- [9] Veit G, Xu H, Dreano E, Avramescu RG, Bagdany M, Beitel LK, et al. Structure-guided combination therapy to potentially improve the function of mutant CFTRs. *Nat Med*. 2018;24:1732-42.
- [10] Okiyoneda T, Barriere H, Bagdany M, Rabeh WM, Du K, Hohfeld J, et al. Peripheral protein quality control removes unfolded CFTR from the plasma membrane. *Science*. 2010;329:805-10.
- [11] Veit G, Avramescu RG, Perdomo D, Phuan PW, Bagdany M, Apaja PM, et al. Some gating potentiators, including VX-770, diminish  $\Delta F508$ -CFTR functional expression. *Sci Transl Med*. 2014;6:246ra97.
- [12] Namkung W, Thiagarajah JR, Phuan PW, Verkman AS. Inhibition of  $Ca^{2+}$ -activated  $Cl^{-}$  channels by gallotannins as a possible molecular basis for health benefits of red wine and green tea. *FASEB J*. 2010;24:4178-86.
- [13] Bagdany M, Veit G, Fukuda R, Avramescu RG, Okiyoneda T, Baaklini I, et al. Chaperones rescue the energetic landscape of mutant CFTR at single molecule and in cell. *Nat Commun*. 2017;8:398.
- [14] Schnur A, Premchandrar A, Bagdany M, Lukacs GL. Phosphorylation-dependent modulation of CFTR macromolecular signalling complex activity by cigarette smoke condensate in airway epithelia. *Sci Rep*. 2019;9:12706.

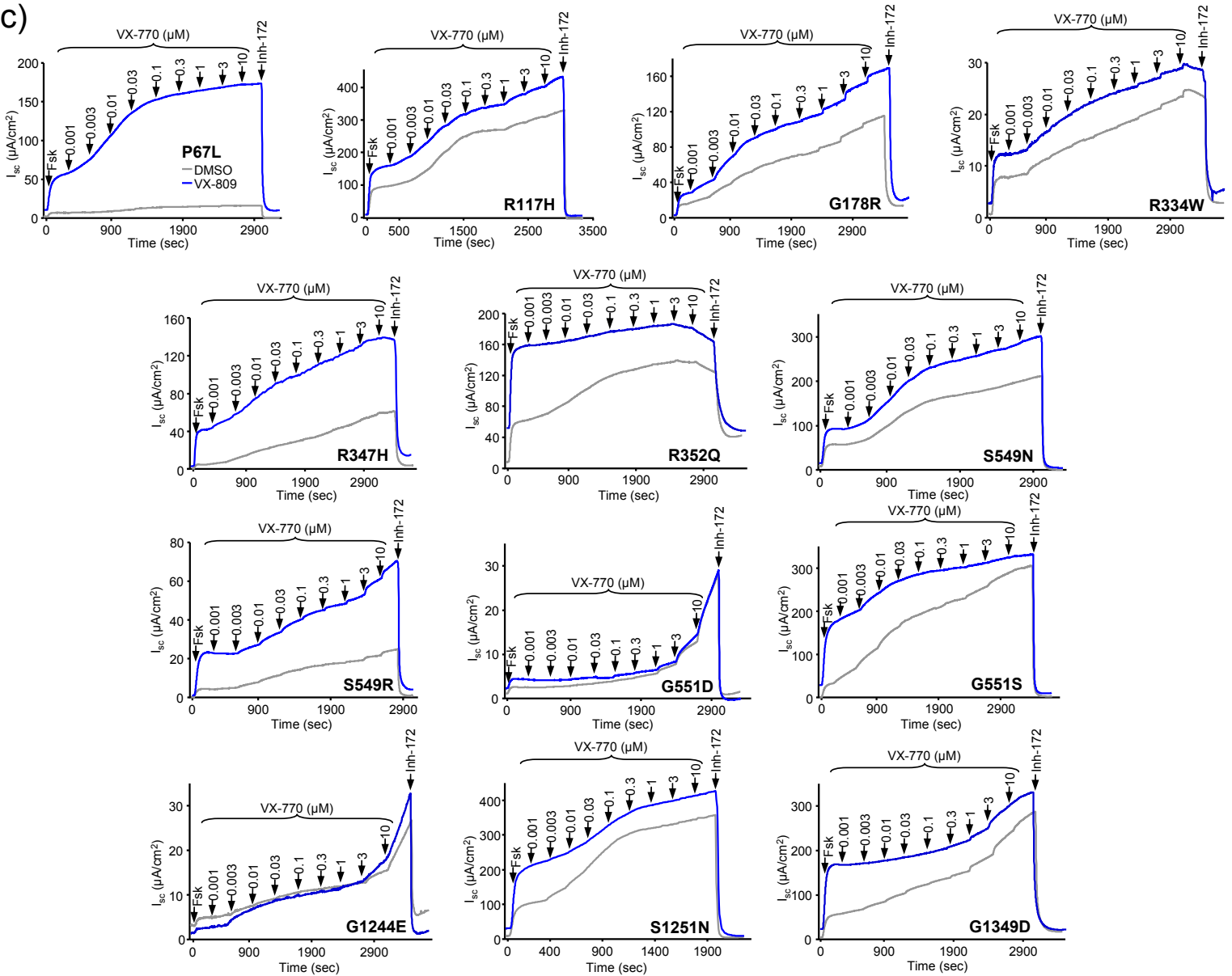
a)



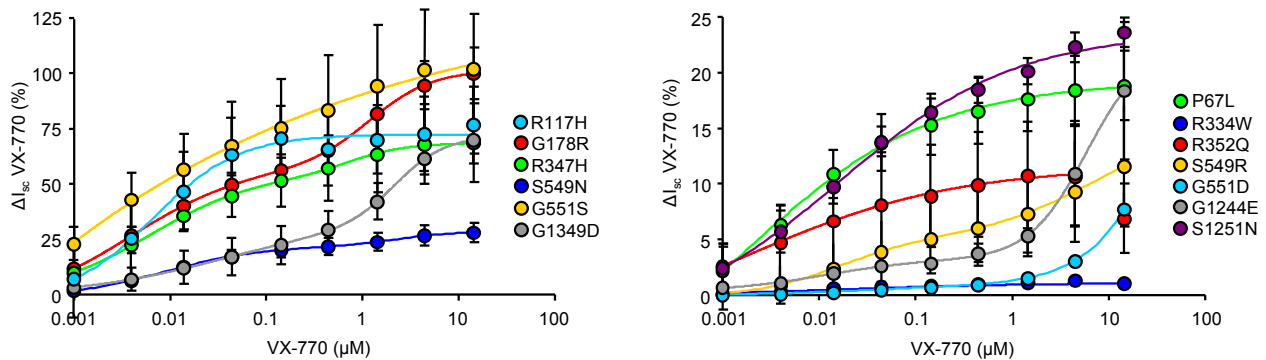
b)



c)

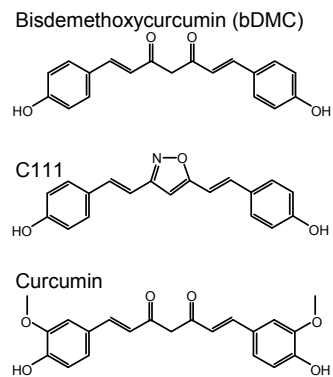
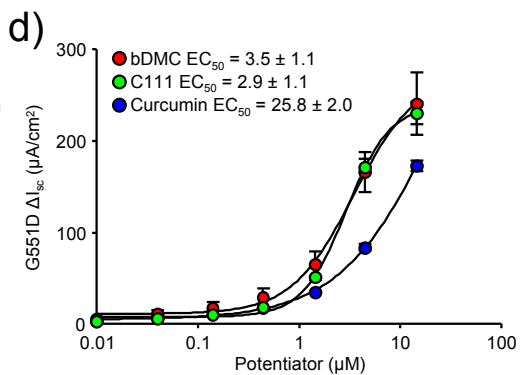
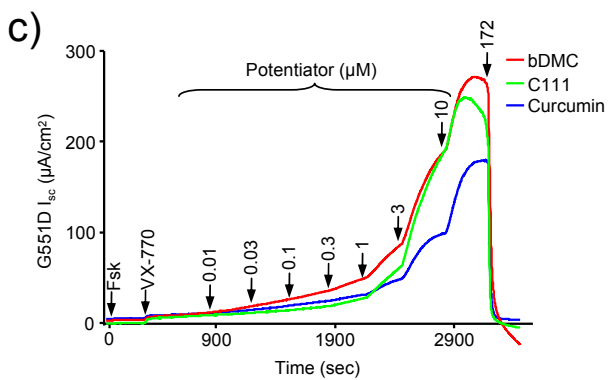
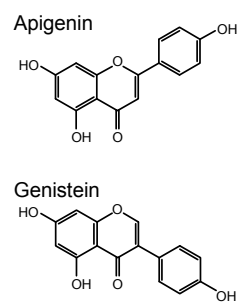
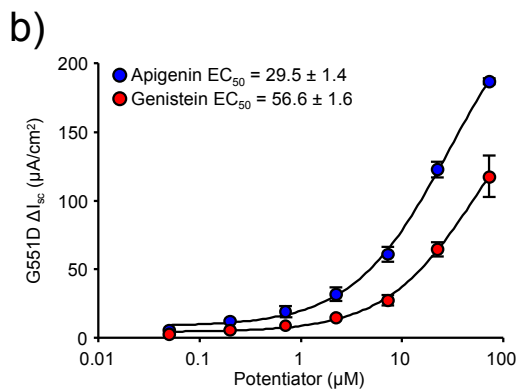
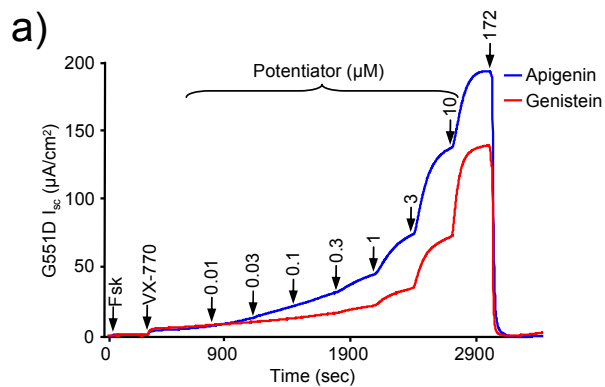


d)

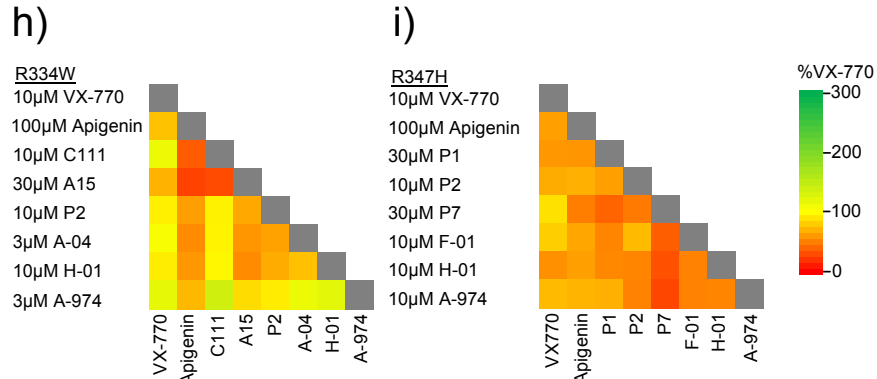
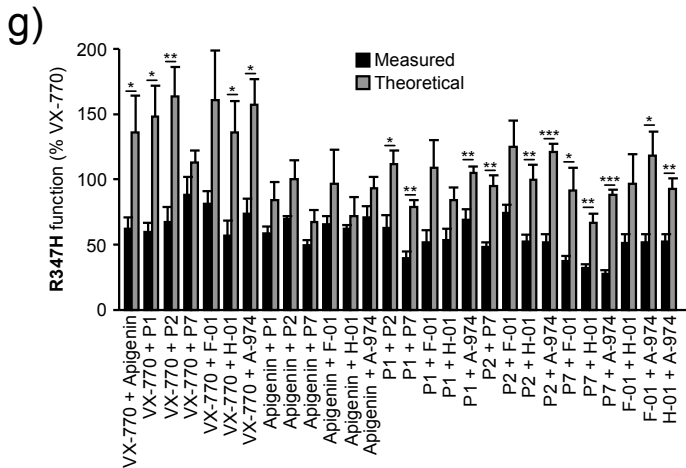
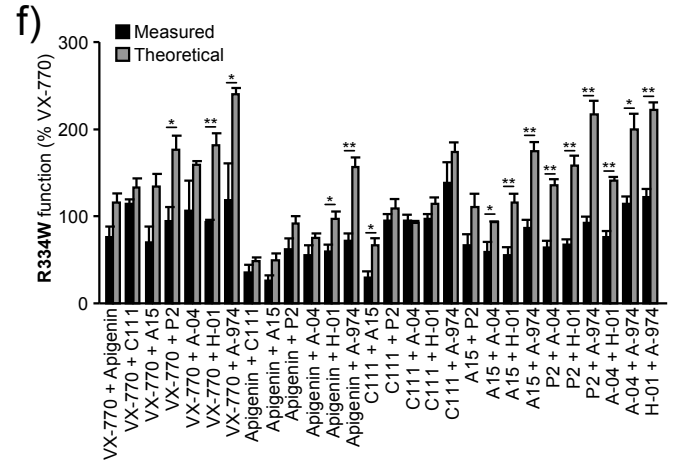
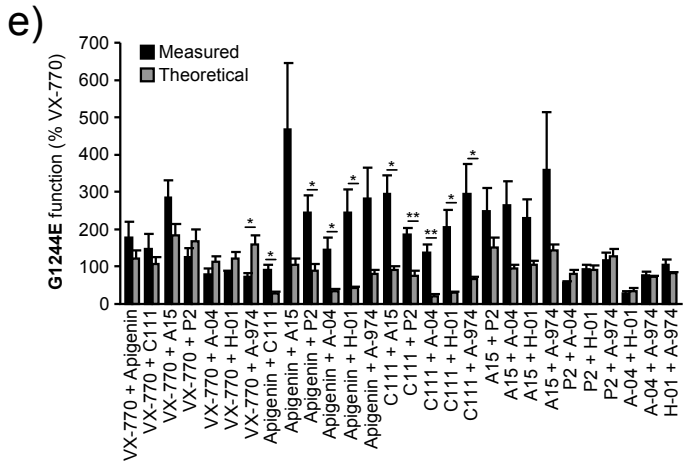
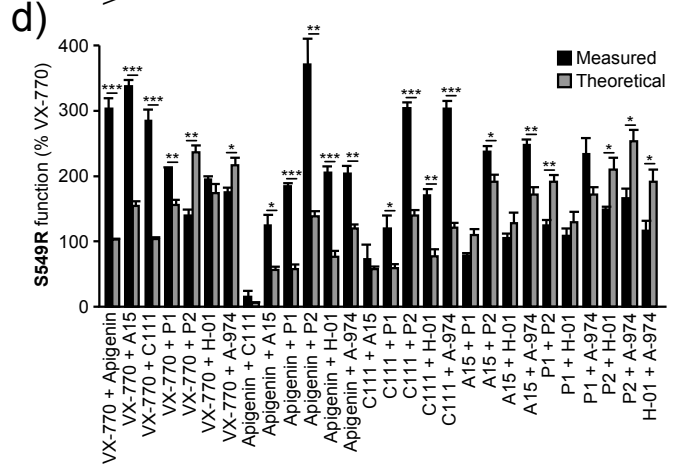
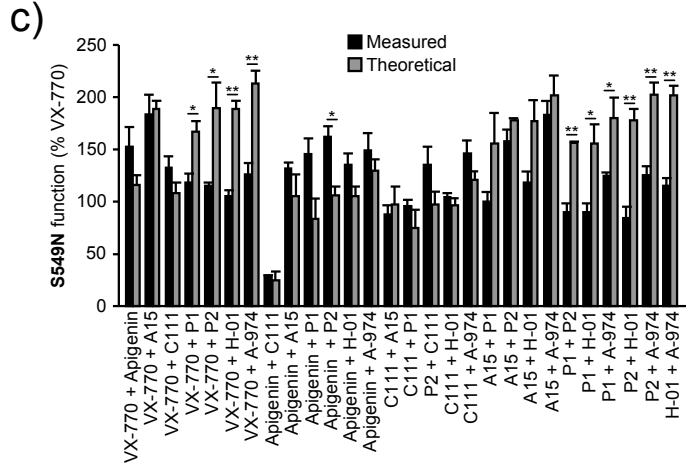
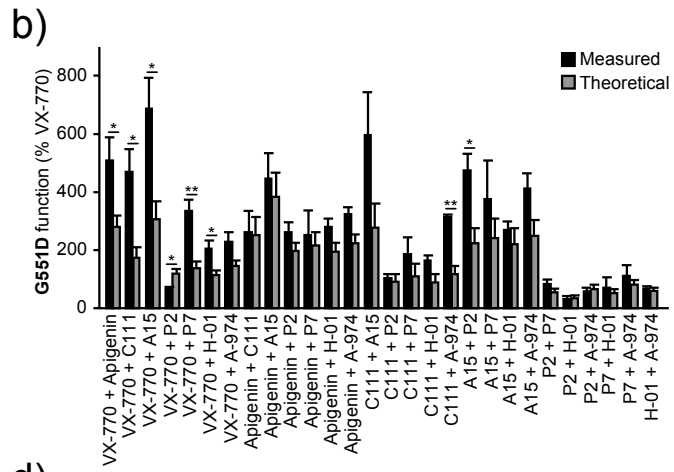
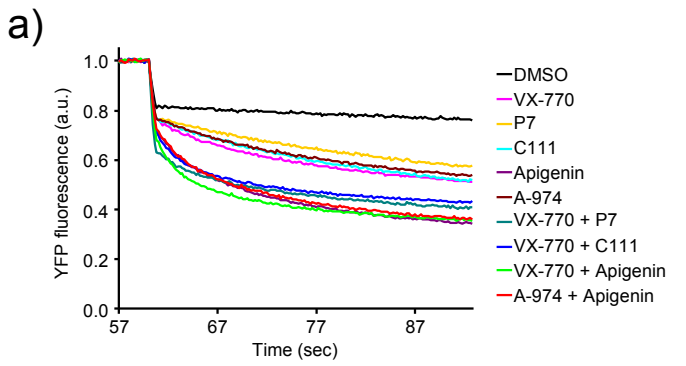


**Supplementary Fig. 1. Characterization of CFTR mutants and their response to VX-770.**

(a) Immunoblot of CFBE expressing inducible CFTR mutants with an extracellular 3HA tag under the control of the TetON doxycycline regulated transactivator induced for  $\geq 3$  days. CFTR was visualized with anti-HA antibody, and anti- $\text{Na}^+/\text{K}^+$ -ATPase antibody served as loading control. The empty arrowheads show the mature, complex glycosylated CFTR (C-band), the filled arrowheads show the immature, core glycosylated protein (B-band), and the amount of protein loaded is indicated. (b) Mutant CFTR mRNA expression in CFBE determined by qPCR and expressed as percent of WT-CFTR mRNA level ( $n = 3-4$ ). Data are means  $\pm$  SEM. (c) Representative  $I_{sc}$  traces of CFTR mutant response to forskolin (20  $\mu\text{M}$ ) and increasing concentrations of VX-770 in CFBE with or without VX-809 treatment (3  $\mu\text{M}$ , 24 hours). Measurements were performed in the presence of a basolateral-to-apical chloride gradient after basolateral permeabilization with amphotericin B (100  $\mu\text{M}$ ) and inhibition of the epithelial sodium channel ENaC with amiloride (100  $\mu\text{M}$ ). Specificity of the currents was confirmed by inhibition with CFTR<sub>inh</sub>-172 (Inh-172, 20  $\mu\text{M}$ ). (d) Dose-response of VX-770 potentiation of the indicated mutants determined in forskolin-stimulated CFBE after correction with VX-809 (3  $\mu\text{M}$ , 24 hours). The  $\Delta I_{sc}$  values for the potentiator effect are expressed as percentage of the forskolin-induced WT-CFTR current ( $n = 3$ ). Data in b and d are means  $\pm$  SEM.



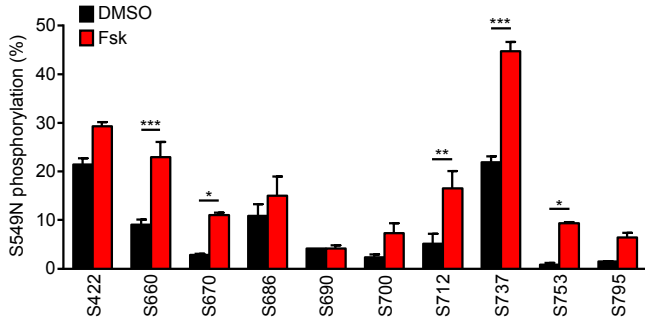
**Supplementary Fig. 2.** Identification of genistein and curcumin analogs. **(a, b)** Representative traces (a) and quantification (n = 3, b) of genistein and apigenin dose-response on the  $I_{sc}$  of G551D-CFTR in the presence of forskolin (20  $\mu$ M) and VX-770 (3  $\mu$ M). **(c, d)** Representative traces (c) and quantification (n = 3, d) of the dose-response of curcumin, C111 and bDMC on the  $I_{sc}$  of G551D-CFTR in presence of forskolin (20  $\mu$ M) and VX-770 (3  $\mu$ M).  $I_{sc}$  measurements were performed in CFBE in the presence of a basolateral-to-apical chloride gradient after basolateral permeabilization with amphotericin B (100  $\mu$ M) and inhibition of the epithelial sodium channel ENaC with amiloride (100  $\mu$ M). Data in b and d are means  $\pm$  SEM.



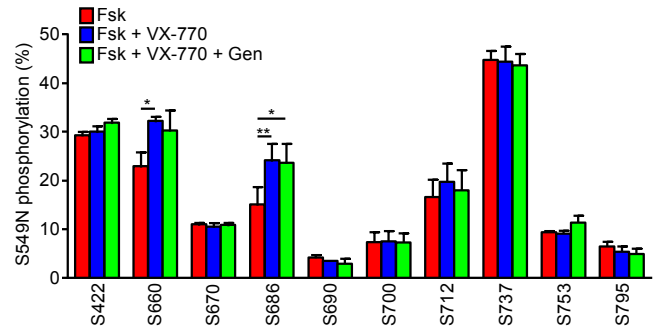


**Supplementary Fig. 3.** The effect of dual potentiator combinations on the function of CFTR mutants in CFBE. **(a-g)** Representative traces (a) and quantification of G551D (b), S549N (c), S549R (d), G1244E (e), R334W (f) or R347H (g) function, measured by halide sensitive YFP quenching assay upon dual potentiator exposure in comparison to the calculated additivity of single potentiator effects (n = 3-4). The YFP quenching kinetics were determined in response to extracellular iodide addition in the presence of forskolin (10  $\mu$ M), IBMX (250  $\mu$ M), cpt-cAMP (250  $\mu$ M), and indicated potentiator combinations and are plotted as percentage of 3  $\mu$ M VX-770 potentiation. The same data, depicted as heat map, is shown in Fig. 3a. **(h, i)** Heat map of the effect of potentiator combinations on the PKA-activated function of R334W- (h) and R347H-CFTR (i) expressed in CFBE (n = 3-4). Data in b-g are means  $\pm$  SEM. A-974 - ABBV-974, \* $P$  < 0.05, \*\* $P$  < 0.01, \*\*\* $P$  < 0.001 by unpaired, two-tailed Student's  $t$ -test.

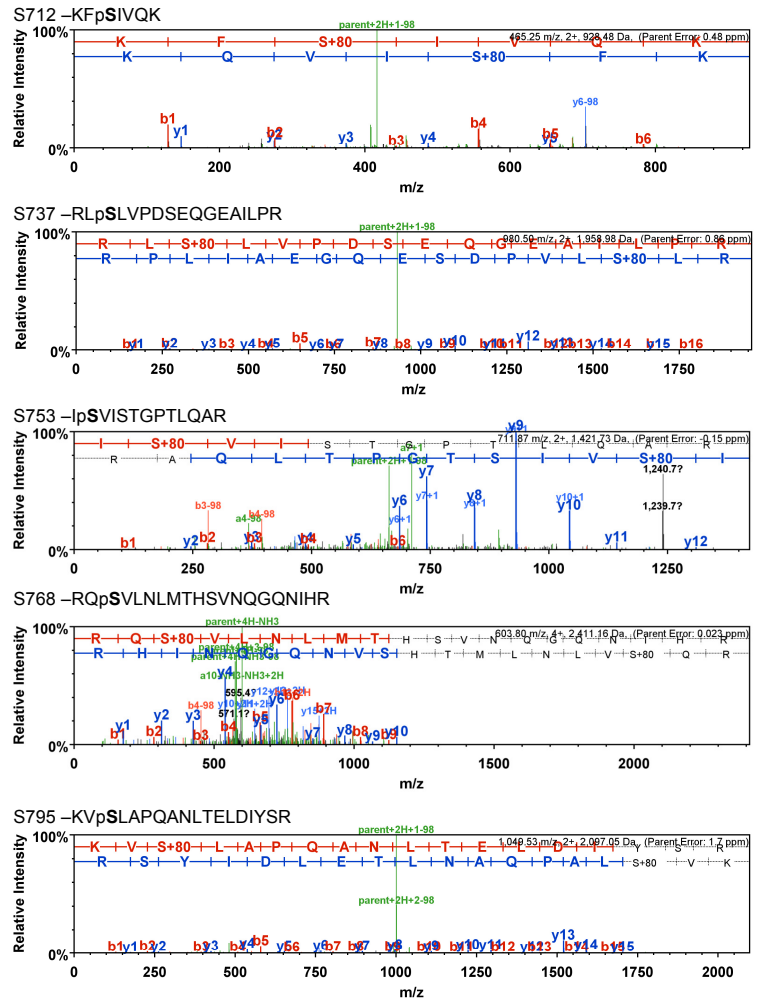
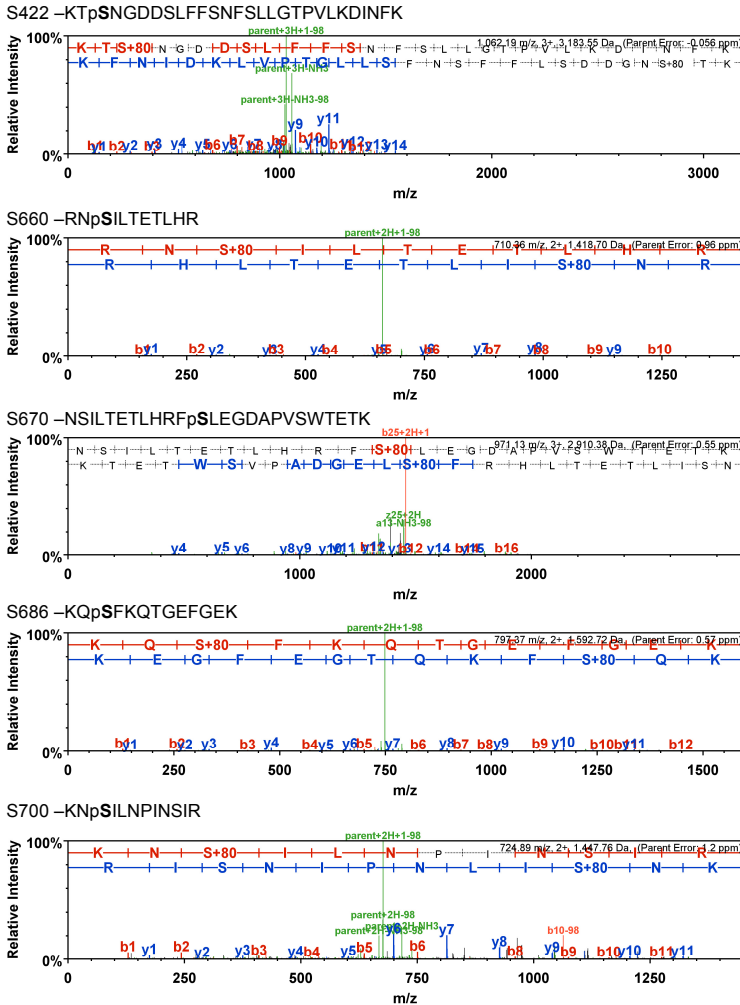
a)



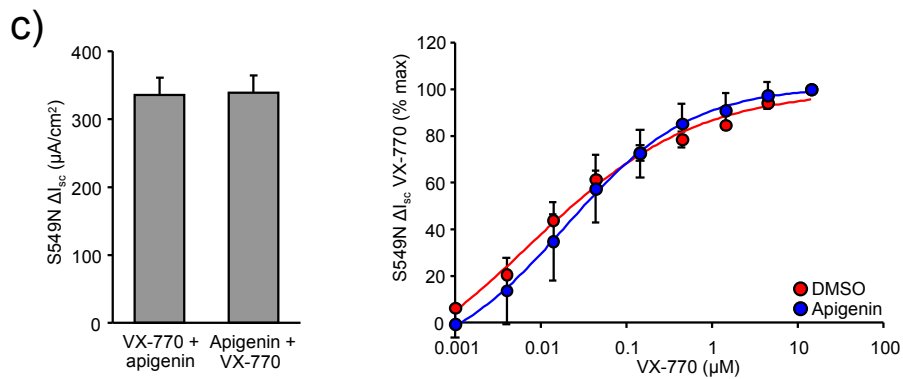
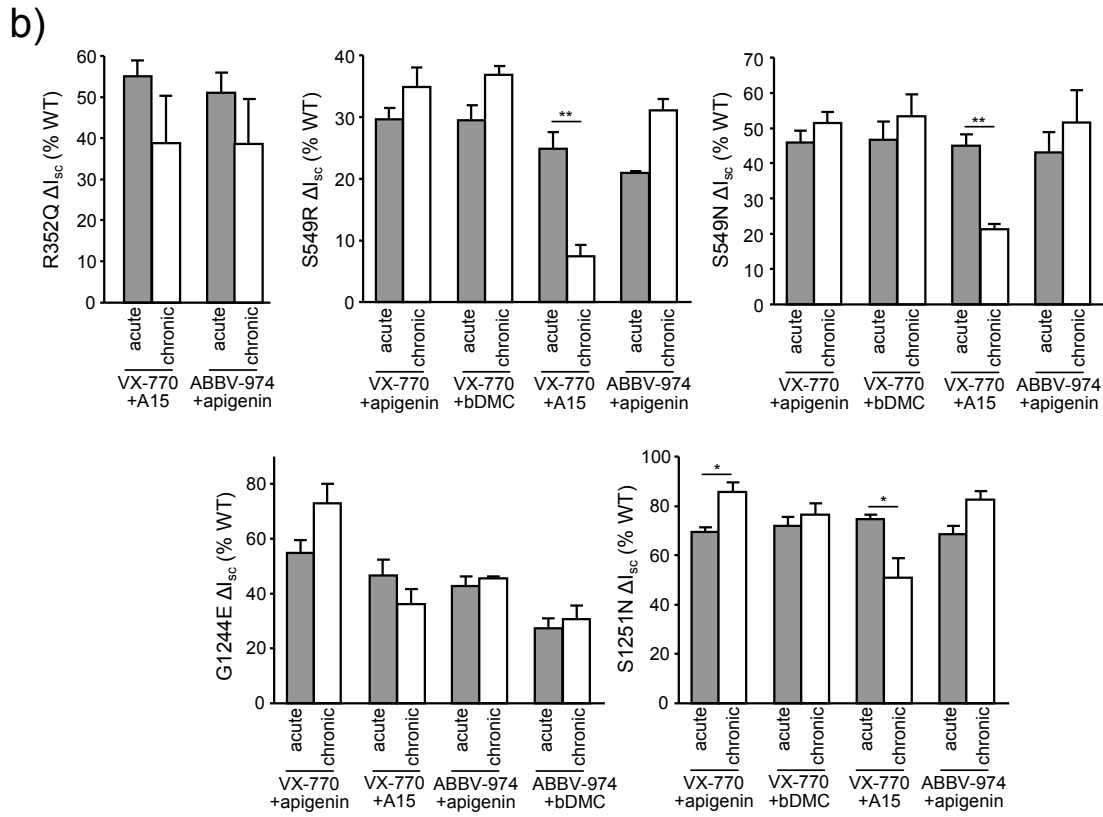
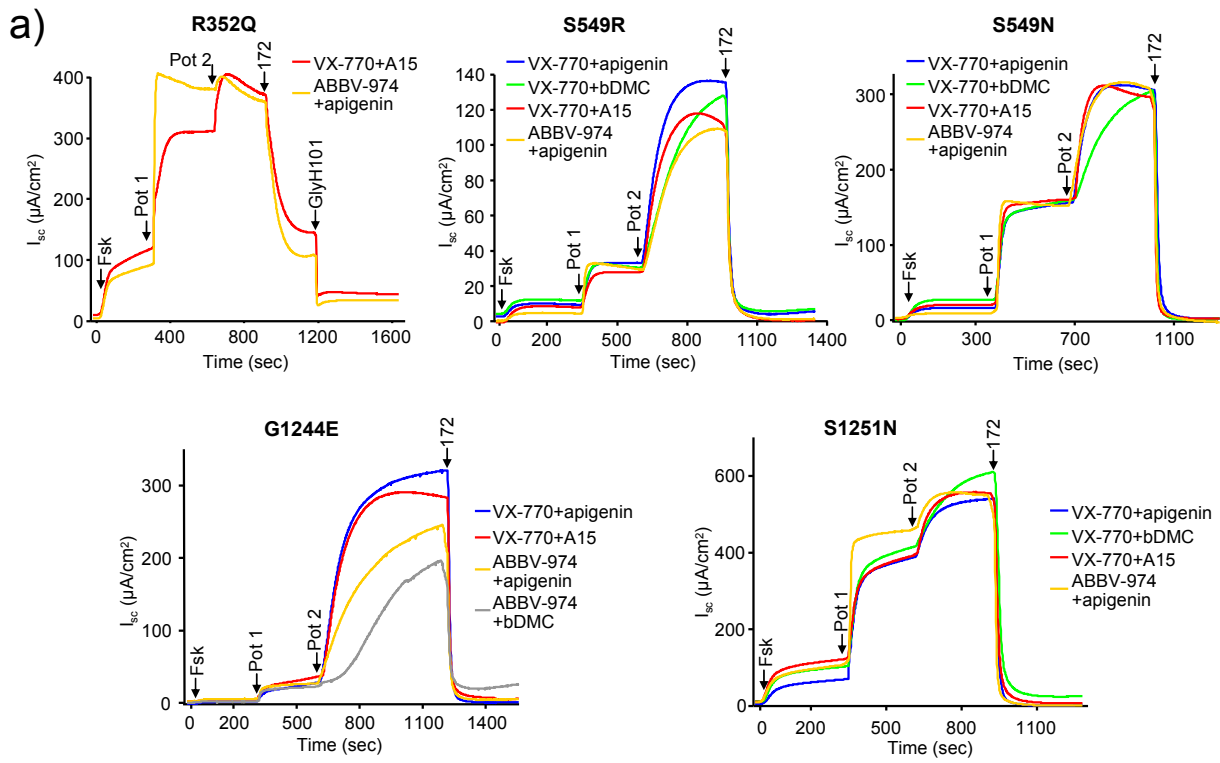
b)



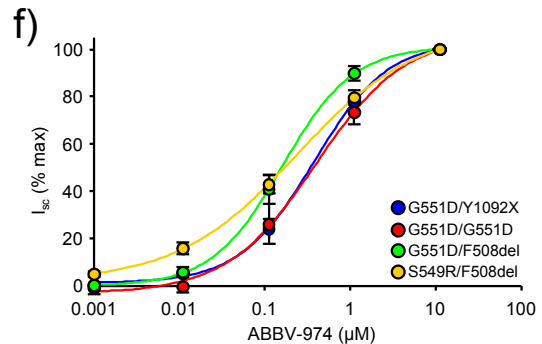
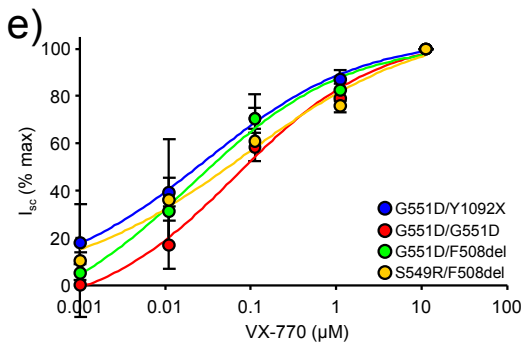
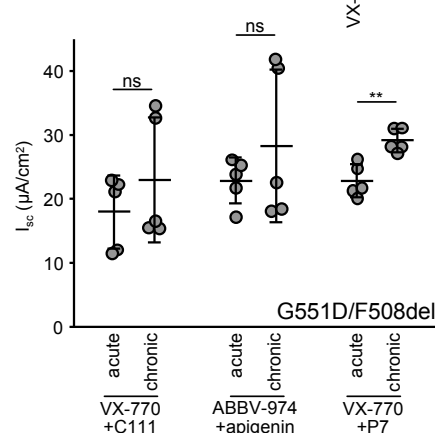
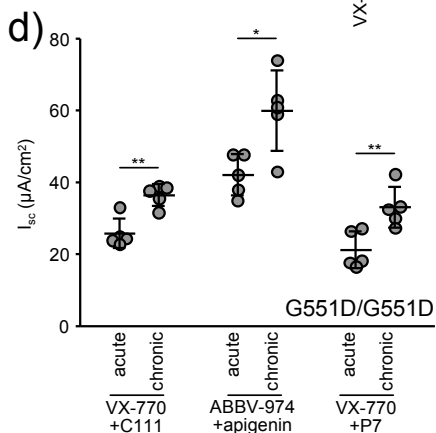
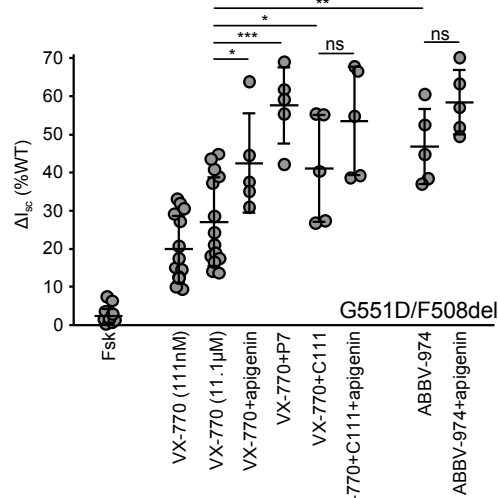
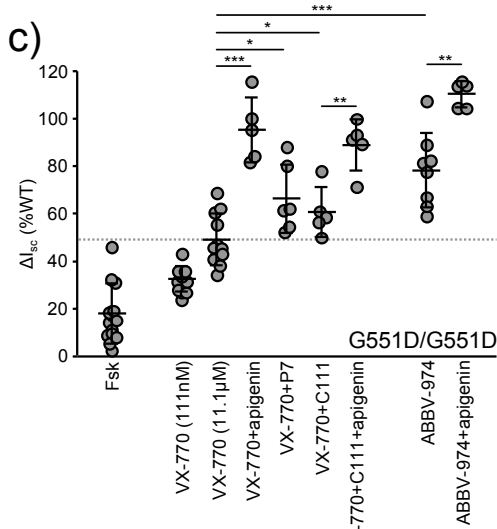
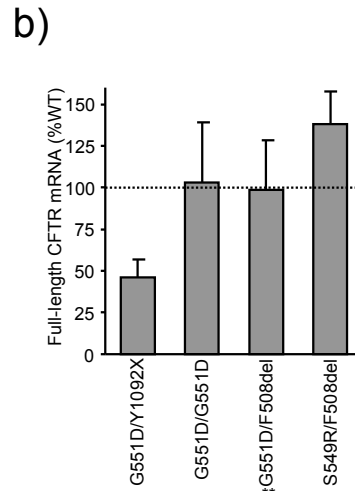
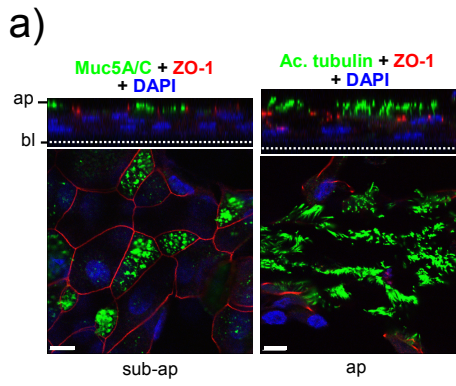
c)



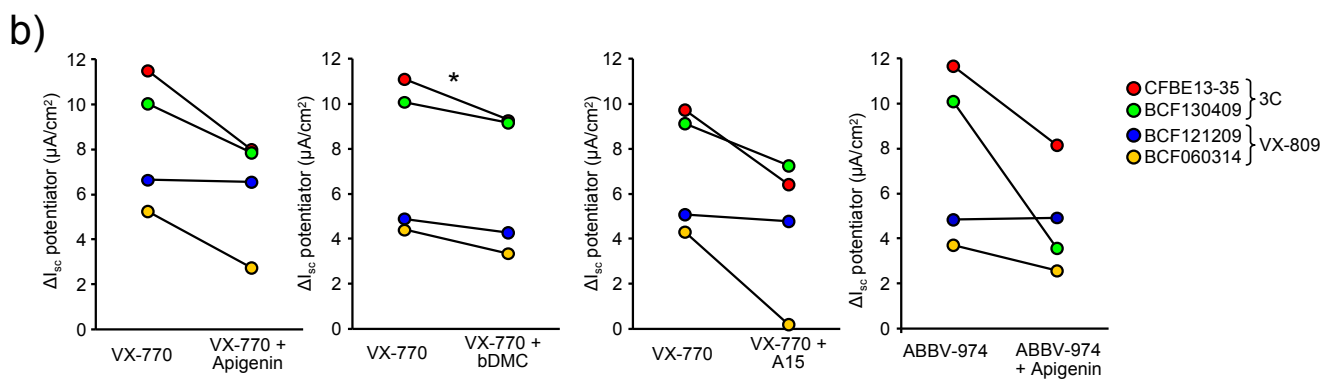
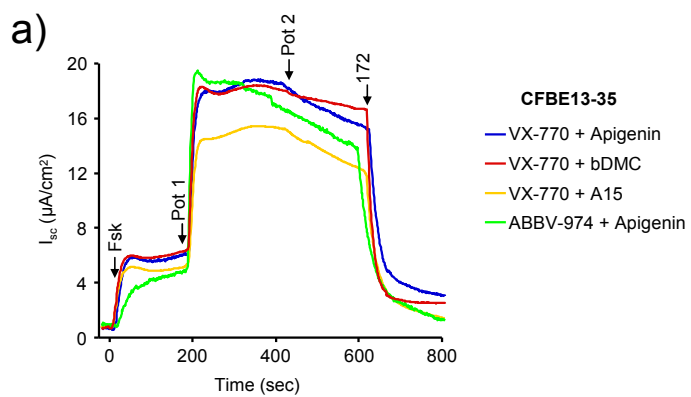
**Supplementary Fig. 4.** Dual potentiator treatment does not substantially alter the CFTR phospho-occupancy. **(a, b)** In vivo phospho-occupancy of the PKA consensus sites in S549N-CFTR expressed in CFBE cells. Relative phosphorylation (%) at PKA consensus sites in S549N-CFTR upon DMSO or forskolin (20 $\mu$ M, 5 min) treatment (a), forskolin alone and VX-770 (3 $\mu$ M, 5 min) or VX-770 + genistein (Gen, 50 $\mu$ M, 5 min) in the presence of forskolin (b). Data are means  $\pm$  SEM of at least three independent experiments. \* $P$  < 0.05, \*\* $P$  < 0.01, \*\*\* $P$  < 0.001 by unpaired, two-tailed Student's  $t$ -test. **(c)** MS/MS fragmentation spectra of phosphorylated peptide sequences. Representative peptide fragmentation spectra from each identified PKA consensus phosphosites as visualized in the Scaffold Viewer software. The fragment ions can either be b- (blue) or y-ions based on the charge retention at the N- or C-terminal fragment, respectively. Fragmentation evidence from both b- and/or y- ions, labelled intensity peaks, and amino acid assignment reflects upon the good spectral quality and higher confidence of phosphosite identification. The peptide sequence is indicated above each spectrum, with the phosphosite marked as pS.



**Supplementary Fig. 5.** Potentiator combinations rescue the function of CFTR gating mutants in CFBE cells. **(a)** The effect of the indicated single potentiators or potentiator combinations on the  $I_{sc}$  of R352Q-, S549R-, S549N-, G1244E- and S1251N-CFTR.  $I_{sc}$  was measured in presence of a basolateral-to-apical chloride gradient after basolateral permeabilization with amphotericin B (100  $\mu$ M) and inhibition of the epithelial sodium channel ENaC with amiloride (100  $\mu$ M). CFTR activity was stimulated with forskolin (20  $\mu$ M) followed by VX-770 (10  $\mu$ M) or ABBV-974 (10  $\mu$ M) and apigenin (50  $\mu$ M), bDMC (10  $\mu$ M) or A15 (50  $\mu$ M). **(b)** Comparison between the acute and chronic (24 hours, VX-770 - 1  $\mu$ M, ABBV-974 - 3  $\mu$ M, bDMC - 10  $\mu$ M, apigenin and A15 - 50  $\mu$ M) potentiator effect on the  $I_{sc}$  of acutely forskolin-stimulated R352Q-, S549R-, S549N-, G1244E- and S1251N-CFTR (n = 3). **(c)** Effect of order-of-addition on the efficacy of S549N potentiation (10  $\mu$ M VX-770, 50  $\mu$ M apigenin) (left panel, n = 3) and potency of VX-770 in the presence or absence of apigenin (50  $\mu$ M) (right panel, n = 3). Data in b and c are means  $\pm$  SEM. \* $P$  < 0.05 by unpaired, two-tailed Student's  $t$ -test.



**Supplementary Fig. 6.** Dual potentiator-mediated rescue of G551D- and S549R-CFTR function in human nasal epithelia (HNE). **(a)** HNE with  $CFTR^{WT/WT}$  genotype were expanded using CR, followed by differentiation on filter supports under ALI culture for 3 weeks. Epithelia were immunostained for markers of goblet cells (mucin5AC, Muc5A/C, green), ciliated cells (acetylated tubulin, Ac. tubulin, green) and tight junctions (protein zonula occludens-1, ZO-1, red) and visualized by laser confocal fluorescence microscopy. Nuclei were stained with DAPI. The transverse (xz, top) and horizontal (xy, bottom) optical sections are shown. Dotted lines indicate the filter membrane. Ap - apical, bl - basolateral, size bar:10  $\mu$ m. **(b)** CFTR mRNA expression in HNE determined by qPCR and expressed as percent of WT-CFTR mRNA level in HNE from five donors (n = 3). Data are means  $\pm$  SEM. **(c)** Quantification of the forskolin- (Fsk) and potentiator stimulated currents ( $\Delta I_{sc}$ ) in HNE with  $CFTR^{G551D/G511D}$  (left panel) or  $CFTR^{G551D/F508del}$  (right panel) genotype expressed as percentage of WT-CFTR currents in HNE from five donors.  $I_{sc}$  was measured with equimolar chloride concentrations in both chambers. After ENaC inhibition, HNE were exposed to forskolin (20  $\mu$ M), increasing concentrations of VX-770 or ABBV-974, followed by apigenin (50  $\mu$ M), C111 (10  $\mu$ M) or P7 (50  $\mu$ M). **(d)** Comparison between the acute and chronic potentiator effect (24 hours, VX-770 and ABBV-974 - 1  $\mu$ M, bDMC - 10  $\mu$ M, apigenin and P7 - 50  $\mu$ M) on the  $I_{sc}$  of forskolin-stimulated  $CFTR^{G551D/G511D}$  (left panel) or  $CFTR^{G551D/F508del}$  (right panel) HNE. Data in c-d are values from individual filters; solid lines indicate means  $\pm$  SEM. **(e, f)** Dose-response of VX-770 (e) and ABBV-974 (f) for the potentiation of the indicated CFTR genotypes determined in forskolin-stimulated HNE. The  $I_{sc}$  values for the potentiator effect are expressed as percentage of highest potentiator concentration (n = 3-15). Data are means  $\pm$  SEM. \* $P$  < 0.05, \*\* $P$  < 0.01, \*\*\* $P$  < 0.001 by unpaired, two-tailed Student's  $t$ -test.



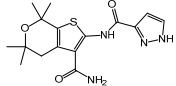
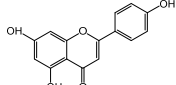
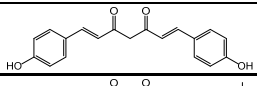
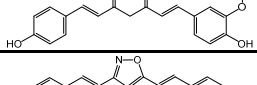
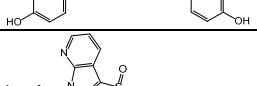
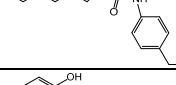
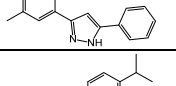
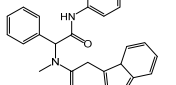
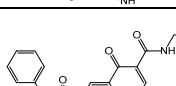
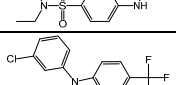
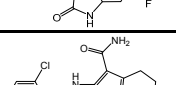
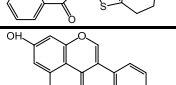
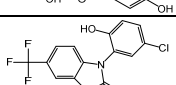
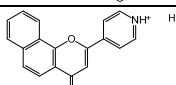
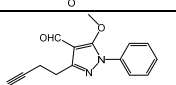
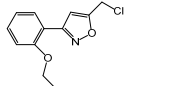
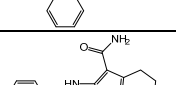


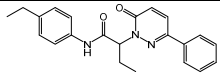
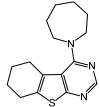
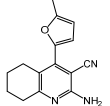
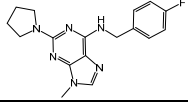
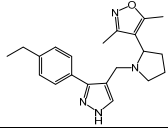
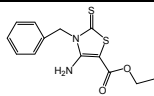
**Supplementary Fig. 7.** Acute effect of potentiator combination on the CFTR channel function in *CFTR*<sup>AF508/AF508</sup> HBE isolated from 4 individuals. HBE cells were differentiated for  $\geq 4$  weeks at ALI followed by correction with VX-809 (3 $\mu$ M, 24h) or 3C (3 $\mu$ M VX-809 + 10 $\mu$ M 4172 + 10 $\mu$ M 3151, 24h) [9]. Intact monolayers were measured in an Ussing setup with equimolar chloride concentration in both chambers in the presence of amiloride (100 $\mu$ M). After activation with forskolin (20 $\mu$ M) cells were potentiated with potentiator 1 (3 $\mu$ M VX-770 or ABBV-974) and potentiator 2 (50 $\mu$ M Apigenin, 50 $\mu$ M A15 or 10 $\mu$ M bDMC) as indicated, followed by inhibition with CFTR<sub>inh</sub>-172 (172, 20 $\mu$ M). **(a)** Representative traces. **(b)** Quantification of the potentiator effect. \* $P < 0.05$  by unpaired, two-tailed Student's *t*-test.

**Supplementary Table 1: 470M/V status of mutants.**

<b>Mutant</b>	<b>M/V</b>
P67L	M
R117H	V
G178R	V
R334W	V
R347H	M
R352Q	M
S549N	M
S549R	M
G551D	M
G551S	V
G1244E	V
S1251N	V
G1349D	V

**Supplementary Table 2: Efficacy of single potentiators.** Increase of mutant function by indicated potentiators expressed as percent of 3  $\mu$ M VX-770 effect was determined by halide sensitive YFP assay. Bolded, values for potentiators used in subsequent experiments.

	<b>R334W (n = 3)</b>	<b>R347H (n = 4)</b>	<b>S549N (n = 4)</b>	<b>S549R (n = 3)</b>	<b>G551D (n = 3)</b>	<b>G1244E (n = 3)</b>	
	Mean $\pm$ SEM	Mean $\pm$ SEM	Mean $\pm$ SEM	Mean $\pm$ SEM	Mean $\pm$ SEM	Mean $\pm$ SEM	
<b>ABBV-974</b> (10 $\mu$ M)	<b>163.5 <math>\pm</math> 27.2</b>	<b>101.7 <math>\pm</math> 4.2</b>	<b>141.8 <math>\pm</math> 14</b>	<b>179.1 <math>\pm</math> 15.7</b>	<b>224.3 <math>\pm</math> 14.5</b>	<b>151 <math>\pm</math> 26.5</b>	
<b>Apigenin</b> (50 $\mu$ M)	<b>18.1 <math>\pm</math> 8</b>	<b>55.5 <math>\pm</math> 8.5</b>	<b>29.8 <math>\pm</math> 4.1</b>	<b>1.7 <math>\pm</math> 0.9</b>	<b>30.3 <math>\pm</math> 6.7</b>	<b>52.1 <math>\pm</math> 13.2</b>	
<b>bDMC</b> (10 $\mu$ M)	13.5 $\pm$ 5.5	14.4 $\pm$ 3.1	12.3 $\pm$ 9	5.8 $\pm$ 3.2	14.1 $\pm$ 6.6	10.5 $\pm$ 5	
<b>C110</b> (10 $\mu$ M)	5.2 $\pm$ 3.2	11.9 $\pm$ 3.3	2.2 $\pm$ 5.7	46.8 $\pm$ 3.1	8.1 $\pm$ 0.7	11.5 $\pm$ 0.1	
<b>C111</b> (10 $\mu$ M)	<b>28.3 <math>\pm</math> 9</b>	34.6 $\pm$ 8.1	<b>11.4 <math>\pm</math> 3.8</b>	<b>4.3 <math>\pm</math> 0.3</b>	<b>23.6 <math>\pm</math> 6.4</b>	<b>17.1 <math>\pm</math> 4.3</b>	
<b>A15</b> (50 $\mu$ M)	<b>50.3 <math>\pm</math> 14.1</b>	35.1 $\pm$ 9	<b>120.4 <math>\pm</math> 3.4</b>	<b>167.3 <math>\pm</math> 27.9</b>	<b>180.8 <math>\pm</math> 33.6</b>	<b>134.8 <math>\pm</math> 36.3</b>	
<b>P1</b> (10 $\mu$ M)	53.8 $\pm$ 4.9	<b>78.9 <math>\pm</math> 12</b>	<b>37.4 <math>\pm</math> 9.2</b>	<b>27.5 <math>\pm</math> 8.7</b>	33.8 $\pm$ 5.8	17.9 $\pm$ 5.8	
<b>P2</b> (3 $\mu$ M)	<b>82.2 <math>\pm</math> 7.2</b>	<b>103.5 <math>\pm</math> 23.2</b>	<b>83.1 <math>\pm</math> 4.8</b>	<b>126.1 <math>\pm</math> 14.1</b>	<b>66.4 <math>\pm</math> 1</b>	<b>45.3 <math>\pm</math> 14.5</b>	
<b>P3</b> (3 $\mu$ M)	33 $\pm$ 1.6	-23.2 $\pm$ 3.7	-11.5 $\pm$ 10.3	-23.1 $\pm$ 1	4.9 $\pm$ 0.6	0.7 $\pm$ 1.5	
<b>P4</b> (10 $\mu$ M)	44 $\pm$ 1.8	34.9 $\pm$ 10.7	24 $\pm$ 11	-6.5 $\pm$ 1.8	5.3 $\pm$ 1.1	0.4 $\pm$ 1.1	
<b>P5</b> (10 $\mu$ M)	62.8 $\pm$ 11.3	35.5 $\pm$ 8.5	23.8 $\pm$ 7.9	-4.8 $\pm$ 2.9	9.5 $\pm$ 0.6	3.2 $\pm$ 2.8	
<b>P6</b> (50 $\mu$ M)	36.1 $\pm$ 4.6	11 $\pm$ 3	149.1 $\pm$ 39.2	131.9 $\pm$ 14.2	15.2 $\pm$ 2.7	20.5 $\pm$ 4.2	
<b>P7</b> (50 $\mu$ M)	5 $\pm$ 13.2	<b>64 <math>\pm</math> 8.9</b>	3.9 $\pm$ 6.7	36.1 $\pm$ 11.6	<b>65.4 <math>\pm</math> 5.8</b>	14.3 $\pm$ 5.6	
<b>P8</b> (50 $\mu$ M)	28 $\pm$ 0.9	8.5 $\pm$ 3.5	32.8 $\pm$ 13.4	5.6 $\pm$ 1.6	-0.2 $\pm$ 0.4	6.5 $\pm$ 2.2	
<b>P9</b> (50 $\mu$ M)	1.4 $\pm$ 4.5	7.8 $\pm$ 2.9	48.2 $\pm$ 21.9	7.5 $\pm$ 0.8	-0.7 $\pm$ 0.5	1.9 $\pm$ 1.7	
<b>P10</b> (10 $\mu$ M)	8.6 $\pm$ 14.6	-2.3 $\pm$ 2.5	6.1 $\pm$ 5.2	3.2 $\pm$ 11	1.3 $\pm$ 1.1	1.1 $\pm$ 1.6	
<b>P12</b> (3 $\mu$ M)	52.1 $\pm$ 1.7	34.3 $\pm$ 4.9	-12.2 $\pm$ 2	-15.9 $\pm$ 6.1	7.8 $\pm$ 0.8	2.5 $\pm$ 3.6	

	<b>R334W (n = 3)</b>	<b>R347H (n = 4)</b>	<b>S549N (n = 4)</b>	<b>S549R (n = 3)</b>	<b>G551D (n = 3)</b>	<b>G1244E (n = 3)</b>	
	Mean ± SEM	Mean ± SEM	Mean ± SEM	Mean ± SEM	Mean ± SEM	Mean ± SEM	
<b>C-01</b> (10 μM)	91 ± 17.3	42.6 ± 6.1	-4.4 ± 7.1	-5.9 ± 3.6	20.4 ± 1.5	3.7 ± 6.6	
<b>D-01</b> (10 μM)	26.6 ± 15.4	8.8 ± 4.2	3.6 ± 3.2	8.1 ± 10.2	0.2 ± 0.1	-6.5 ± 2.2	
<b>E-01</b> (10 μM)	28.5 ± 12.2	13.1 ± 3.5	6.4 ± 11.4	2.1 ± 4.8	1 ± 0.2	-10.2 ± 2.6	
<b>F-01</b> (10 μM)	77.6 ± 13.7	<b>82.5 ± 6.5</b>	47 ± 10.2	47 ± 3.5	41 ± 1.4	22.1 ± 8.6	
<b>H-01</b> (10 μM)	<b>70.3 ± 12.2</b>	85.5 ± 8	<b>91.4 ± 7.3</b>	<b>150 ± 22.6</b>	<b>71.6 ± 8.7</b>	<b>19.3 ± 8.7</b>	
<b>A-04</b> (3 μM)	<b>96.2 ± 5.8</b>	<b>26.8 ± 4</b>	11 ± 5.1	9.6 ± 9.4	30.9 ± 1.6	<b>11.9 ± 7.3</b>	

**Supplementary Table 3: EC<sub>50</sub> of potentiators.** Dose-response was determined by short-circuit current (I<sub>sc</sub>) measurement or halide-sensitive YFP quenching (YFP) assay. N.d. – not determined.

	<b>R334W</b>	<b>R347H</b>	<b>S549N</b>	<b>S549R</b>	<b>G551D</b>	<b>G1244E</b>
	EC <sub>50</sub> (μM)	EC <sub>50</sub> (μM)	EC <sub>50</sub> (μM)	EC <sub>50</sub> (μM)	EC <sub>50</sub> (μM)	EC <sub>50</sub> (μM)
<b>VX-770 (I<sub>sc</sub>)</b>	0.067	EC <sub>50</sub> (1) = 0.008 EC <sub>50</sub> (2) = 1.55	EC <sub>50</sub> (1) = 0.009 EC <sub>50</sub> (2) = 3.32	EC <sub>50</sub> (1) = 0.014 EC <sub>50</sub> (2) = 9.08	EC <sub>50</sub> (1) = 0.38 EC <sub>50</sub> (2) = 4.86	EC <sub>50</sub> (1) = 0.012 EC <sub>50</sub> (2) = 29.4
<b>VX-770 + 3 μM VX-809 (I<sub>sc</sub>)</b>	0.027	EC <sub>50</sub> (1) = 0.006 EC <sub>50</sub> (2) = 0.76	EC <sub>50</sub> (1) = 0.009 EC <sub>50</sub> (2) = 2.33	EC <sub>50</sub> (1) = 0.016 EC <sub>50</sub> (2) = 7.11	EC <sub>50</sub> (1) = 0.31 EC <sub>50</sub> (2) = 4.78	EC <sub>50</sub> (1) = 0.011 EC <sub>50</sub> (2) = 5.85
<b>VX-770 (YFP)</b>	EC <sub>50</sub> (1) = 0.006 EC <sub>50</sub> (2) = 1.87	0.040	EC <sub>50</sub> (1) = 0.002 EC <sub>50</sub> (2) = 2.07	EC <sub>50</sub> (1) = 0.010 EC <sub>50</sub> (2) = 9.71	EC <sub>50</sub> (1) = 0.046 EC <sub>50</sub> (2) = 6.78	EC <sub>50</sub> (1) = 0.011 EC <sub>50</sub> (2) = 7.02
<b>ABBV-974 (YFP)</b>	0.57	5.82	3.38	3.54	3.31	11.0
<b>Apigenin (YFP)</b>	281.3	14.11	21.3	25.4	291.5	315.5
<b>C111 (YFP)</b>	7.38	n.d.	5.23	>100	22.8	24.6
<b>A15 (YFP)</b>	80.2	n.d.	19.4	83.3	30.6	36.2
<b>P1 (YFP)</b>	n.d.	1.70	8.75	7.38	n.d.	n.d.
<b>P2 (YFP)</b>	n.d.	0.28	1.67	6.37	1.46	1.43
<b>P7 (YFP)</b>	n.d.	23.53	n.d.	n.d.	>100	n.d.
<b>F-01 (YFP)</b>	n.d.	2.03	n.d.	n.d.	n.d.	n.d.
<b>H-01 (YFP)</b>	1.32	5.03	n.d.	n.d.	28.3	6.70
<b>A-04 (YFP)</b>	0.31	n.d.	n.d.	n.d.	n.d.	0.47